Density Functional Study on the Thermal Stabilities of Phenolic Bio-oil Compounds

Alexander Shaw, Xiaolei Zhang*

School of Mechanical and Aerospace Engineering, Queen's University Belfast, Belfast, United Kingdom

Corresponding author:

E-mail: xiaolei.zhang@qub.ac.uk, Tel: +44(0)2890974490

Abstract

Pyrolysis of biomass provides a potential carbon-neutral route to fuels and precursor chemicals through the formation of bio-oil. Lignin accounts for up to 40% of the weight of biomass feedstocks and so the products of lignin deconstruction form a significant portion of the bio-oil. Understanding the thermal stability of bio-oil species is critical for predicting the relationship between product prevalence and pyrolysis temperature, which in turn will allow for greater control of the output of key products. In this work, density functional theory (DFT) was employed to assess the stabilities of key bio-oil compounds by calculating their bond dissociation enthalpies (BDEs). 140 individual bonds across twenty-seven common bio-oil compounds representing eight different bond types were assessed. It was found that the PW6B95 functional can be used as a reliable method for predicting pyrolysis product stability through calculation of functional group BDEs. This is mainly owing to its low mean unsigned error (MUE) (0.5 kcal mol^{-1} = 2.1 kJ mol^{-1}) in predicting BDEs in a test set of six bonds, as well as correct treatment of aromatic substitution effects for phenolic derivatives. The assessment results reflected that the weakest bonds of phenolic bio-oil species were the O-Me and Ph-O bond of the methoxy groups and the O-H bond of hydroxy groups. The weak bond strength exhibited by methoxy group bonds correlates well with reduced presence of guaiacyl and syringyl type species following higher temperature pyrolysis. Conversely, the hydroxy Ph-O and propenyl Ph-C bonds exhibited high BDEs, which is in agreement with the persistent presence of phenol and styrene type species following high temperature pyrolysis.

Keywords: Biomass, Lignin, Pyrolysis, Bio-oil, Bond dissociation enthalpy, Density functional theory

1. Introduction

The increasing energy demands of a rising global population and the continued combustion of fossil fuels are leading towards catastrophic climatic conditions and a worldwide energy shortage. The 2016 global CO_2 emissions from fuel combustion was in excess of 32,000 Mt [1], which is more than double the value around 40 years prior. Utilisation of biomass derived fuels and chemicals would help significantly in reducing anthropogenic CO_2 emissions by providing alternatives to the consumption of traditional fossil fuels. The uptake of atmospheric carbon in equal amounts to its combustion product that is necessary for biomass growth creates the potential for the formation of carbon neutral products. The incorporation of agricultural and forestry waste products as feedstock materials in biofuel production can act to alleviate challenges associated with waste management. Furthermore, use of biomass derived compounds would ease concerns regarding feedstock shortages, owing to the enormous potential for sustainable biomass growth.

One technology that has received significant research interest for the thermochemical conversion of biomass is pyrolysis. During pyrolysis, the feedstock material is thermally decomposed in an inert atmosphere to produce solids, liquids and gas products of varying composition. The ratios of each fraction and their chemical makeup is closely tied to both the identity of the feedstock material, as well as the processing parameters. Within the liquid fraction of the pyrolysis products, termed bio-oil or pyrolysis-oil, many fuel precursor compounds have been identified and bio-oil yields in excess of 50% are commonly reported in the literature [2–4]. This bio-oil is readily subjected to upgrading processes, including hydro-treating, catalytic cracking or several post-gasification treatments [5], to yield transportation fuel compounds comparable to those found in traditional fuels.

One variable that has a significant impact upon the species observed within the bio-oil is the ratio of cellulose, hemi-cellulose and lignin. This in turn is governed by the species of feedstock material. Cellulose is a crystalline polymer with high molecular weight (MW) chains which are formed through the condensation polymerisation of glucopyranose units [6]. Hemicelluloses are a family of branched polysaccharides containing highly variable chains composed of hexoses and pentoses bound together primarily through glycosidic linkages [7]. Hemicellulose exhibits a lower average MW than

cellulose and the variability of the constituent sugar monomers and tendency for crosslinking gives hemicellulose an amorphous structure [8]. Pyrolysis of the celluloses gives rise to the formation of anhydrosugars, including levoglucosan, and furan derivatives, such as hydroxymethyl furfural. A wide array of aldehydes, ketones and carboxylic acids are also produced [9,10]. The structure of lignin exhibits a much greater degree of complexity when compared to the celluloses. A highly cross-linked macromolecule, it is formed through the polymerisation of the monomer units p-coumaryl alcohol, coniferyl alcohol and sinapyl alcohol. Hardwood lignins are mainly guaiacyl based whereas softwoods are formed more primarily of syringyl lignins[11]. It is the structure of these phenolic monomers that gives the products of lignin pyrolysis their highly substituted aromatic nature.

The prevalence of each species in lignin derived pyrolysis oil is further dependent upon the pyrolysis temperature. Phenol and catechol have been shown to be highly stable, with increasing concentrations reported at temperatures up to 800^{O}C [12–15], suggesting that the OH functional group is thermally resilient. Styrene, benzaldehyde and 2-hydroxybenzaldehyde were also been observed at 800^{O}C, following the pyrolysis of two lignin model compounds [14,15]. In all of the aforementioned studies, guaiacol and syringol type products saw marked decreases in concentration with increasing pyrolysis temperature. This can be ascribed to the low thermal stability of C-O ether bonds.

It is well-known that the chemical make-up of bio-oil exhibits a clear dependence on the pyrolysis temperature [16–19]. This suggests that a better understanding of the thermal stability of these product species may allow for prediction of their concentration within the products, as a function of the temperature. A bond dissociation enthalpy (BDE) is the per mole energy requirement for the homolytic cleavage of a given chemical bond [20] and its measurement gives indication as to the strength of a that bond. As strong bonds require more energy to break, calculation of BDEs can provide indication of the thermal stability of a compound.

Whilst not specifically concerned with the component compounds of bio-oil, many works have focussed on the calculation of BDEs of phenolic compounds through the use of computational methods. Brinck et al. [21] calculated the O-H BDEs for 10 substituted phenols at the B3LYP/6-31G** level, finding a reasonable correlation between their predicted results and experimental values. Klein and Lukeš [22], also using the B3LYP functional, calculated the O-H BDEs for 30 *meta*- and *para*-

substituted phenols. They showed that DFT can accurately describe the effect of substituents upon the O-H BDE and that this bond enthalpy can be correlated to the adjacent C-O bond length. Marteau et al. [23] determined the O-H BDEs of several newly synthesised *o*-propenyl substituted phenols, as well the common bio-oil compounds p-cresol, guaiacol and isoeugenol. Using both experimental and computational techniques they concluded that the *o*-propenyl substituent group was the most effective at lowering the O-H BDE. A thorough study performed by Richard et al. [24], involving DFT, high-level post Hartree-Fock methods, and experimental calorimetry, confirmed that the O-H BDEs for cresols are weaker than that of unsubstituted phenol. In order to better understand the effectiveness of a MoO_3 hydrodeoxygenation catalyst, Roman-Leshkov's group [25] calculated the C-O BDEs of guaiacol, phenol, m-cresol, anisole and several monolignols. As may be expected, they found the Ph-OH bond to be the strongest, with all values calculated greater than 100 kcal mol^{-1}. This was followed by the Ph-OMe bonds of around 90 kcal mol^{-1} and the PhO-Me bonds in the region of 50-60 kcal mol^{-1}. The latter bond type also exhibited the largest variation between compounds, suggesting it is the most susceptible to changing substitution patterns.

From the aforementioned studies, and those on larger lignin model compounds [26–29], it is clear that DFT is a suitable method for the determination of BDEs for aromatic species. Nevertheless, the literature is still lacking any in-depth study that provides the BDEs for a range of known lignin-derived phenolic bio-oil compounds. To that end we present the BDEs for twenty-seven phenolic compounds, totalling 140 bonds, in the hopes of initiating a database of bio-oil compounds. Such values are necessary for further developing a clear and quantifiable relationship between compound prevalence and pyrolysis conditions.

2. Methodology

2.1 Computational Details

DFT, a quantum chemical technique that derives the properties of a chemical system as a product of the electron density, is employed to calculate BDEs of the compounds in this work. All calculations were carried out using the quantum chemistry program ORCA (Version 4.0.0.2) [30] which has been employed within the literature for the calculation of BDEs for a range of chemical systems

[31–33]. The hybrid density functionals M06-2X [34], B3LYP [35], PBE0 [36], PW6B95 [37] and B3PW91 [38,39] were chosen for the method comparison study. All further calculations were carried out using the PW6B95 functional. All calculations used the def2-TZVP basis set[40] and the auxiliary def2/J basis [41] as provided in ORCA. Grimme's atom-pairwise dispersion correction with Becke-Johnson damping was applied (D3BJ) [42,43] to all functionals, except in the case of M06-2X, where zero damping was applied, as the former damping scheme is incompatible due to short-range double-counting effects [44]. The RIJCOSX approximation [45] was used to improve convergence rates and has been shown to have minimal effect upon the accuracy of results. Numerical frequencies were used for all calculations owing to the unavailability of analytical frequencies for the meta-GGA functionals.

The BDEs were calculated by Equation 1 [46]:

$$BDE = \Delta_f H_{298}(A) + \Delta_f H_{298}(B) - \Delta_f H_{298}(AB) \quad (1)$$

where A and B denote the radicals resulting from the homolytic fragmentation of the molecule AB. $\Delta_f H_{298}$ is the enthalpy of formation of the species at standard conditions. All terms on the right hand side of Equation 1 are obtained from DFT calculations and from which the BDE is then calculated.

2.2. Methods Selection

2.2.1. Methods Comparison

In order to select an appropriate DFT method, five commonly used hybrid density functionals (M06-2X, B3LYP, PBE0, PW6B95 and B3PW91) were compared for their accuracy in predicting BDEs. For this assessment, BDEs were calculated for seven bond types using each DFT method and compared against equivalent literature values. All empirical enthalpies were the recommended values in the work of Yu-Ran Luo [47], in which BDEs were obtained by collating and assessing a variety of laboratory measurement techniques. The measured bonds in the test set were the toluene Ph-CH_3 bond, phenol Ph-OH and PhO-H bonds, anisole Ph-OCH_3 and PhO-CH_3 bonds, styrene Ph-$CHCH_2$ bond, and benzaldehyde Ph-CHO bond, all chosen to be representative of the types of bonds that arise in the products of lignin pyrolysis. These predicted values, their unsigned error and the mean unsigned errors (MUEs) of each functional are given in Table 1. MUEs are calculated using Equation 2:

$$MUE = \frac{\Sigma_{i=1}^{n} |y_i - x_i|}{n} \quad (2)$$

where y and x are the reference BDE and calculated BDE, respectively, for any compound *i,* and where n is the total number of bonds calculated for each functional.

From the results presented in Table 1, it is clear that the best performing functional in our test was PW6B95, followed by PBE0, with both methods having a MUE of 1.0 kcal mol^{-1} or less. An error of 1.0 kcal mol^{-1} or less (commonly termed as sub-kcal) is considered to be within the limits of experimental accuracy for the measurement of many thermochemical properties and is therefore the target accuracy for predictions of those properties using computational approaches [48]. The worst performing functional was B3LYP, with a MUE of 3.2 kcal mol^{-1}. M06-2X, a functional that has seen significant use over the last decade, did not perform satisfactorily for this investigation, tending to predict BDEs that were too high.

Table 1 Calculated BDEs of each bond for the five DFT methods, their unsigned errors and their MUEs against the reference values. Energies are in kcal mol^{-1}.

Method	Ph-CH_3		Ph-OH		PhO-H		Ph-OCH_3		PhO-CH_3		Ph-$CHCH_2$		Ph-CHO		MUE
	BDE	ΔE	BDE	ΔE	BDE	ΔE	BDE	ΔE	BDE	ΔE	BDE	ΔE	BDE	ΔE	
Ref.	102.0	-	111.3	-	88.0	-	99.2	-	64.2	-	115.2	-	97.6	-	-
M06-2X	102.6	0.6	112.5	1.2	90.3	2.3	102.0	2.8	68.9	4.7	115.1	0.1	99.1	1.5	1.9
B3LYP	98.8	3.2	107.9	3.4	85.3	2.7	95.3	3.9	59.9	4.3	112.4	2.8	95.7	1.9	3.2
PBE0	101.6	0.4	110.7	0.6	85.7	2.3	98.1	1.1	63.7	0.5	114.8	0.4	98.7	1.1	0.9
PW6B95	102.2	0.2	111.1	0.2	86.7	1.3	98.3	0.9	64.7	0.5	114.8	0.4	97.7	0.1	0.5
B3PW91	100.7	1.3	109.9	1.4	85.9	2.1	97.3	1.9	62.3	1.9	114.3	0.9	97.8	0.2	1.4

2.2.2. Method Validation

The products arising from lignin pyrolysis are multiply substituted aromatic species. Within these compounds a complex interplay of inductive, mesomeric and radical stabilisation effects can impact upon bond enthalpies. Simply considering the electron donating ability of a substituent group cannot provide a satisfactory prediction of what changes it will induce in the bond of interest. To further assess the applicability of the PW6B95 functional for predicting the BDEs of substituted phenolic species, the correlation between empirical and calculated values for the O-H bond in eight *meta*- and eight *para*-substituted phenolic derivatives was investigated.

While previous data has been reported regarding the bond dissociation enthalpies for substituted aromatic species, the range of the values presented for a particular species are often larger than the change in BDE that is induced by the presence of the additional substituent group. These discrepancies may in part be caused by the calculation of bond enthalpies using various experimental techniques and under differing conditions. In order to overcome this large variability in reported results, it is the mean of all results given in reference [47] that we correlate against. By averaging the bond enthalpies, the influence of spurious values will be minimised, without dismissing one result in favour of another. *Ortho*-substituted phenols were omitted from this assessment owing to the fact that often a large enough data set was not available for every species in order to produce a reliable mean. All values used are given in the supplementary data.

Figure 1 shows the correlation between the mean reference values and those calculated at the PW6B95/Def2TZVP level. When comparing calculated values versus the reference data for *para*-substituted phenols, a strong correlation is observed, with an R^2 value of 0.97. The *meta*-substituted phenols, while less strongly correlated than the *para*-substituents, still follow a strong trend, with an R^2 value of 0.93. This weaker correlation of the *meta*-substituted species may be explained by the smaller data set provided for the *meta*-substituents and so a spurious value will have a significant impact upon the mean value. In general, deviations from the trend line are on the order of <1.0 kcal mol^{-1} and so any errors in the final BDEs should be minimal. The sub-kcal error in our initial six bond test set and the strong correlation with experimental data for substituted phenols confirm that PW6B95 is a suitable choice of functional for predicting BDEs in lignin derived phenolic compounds.

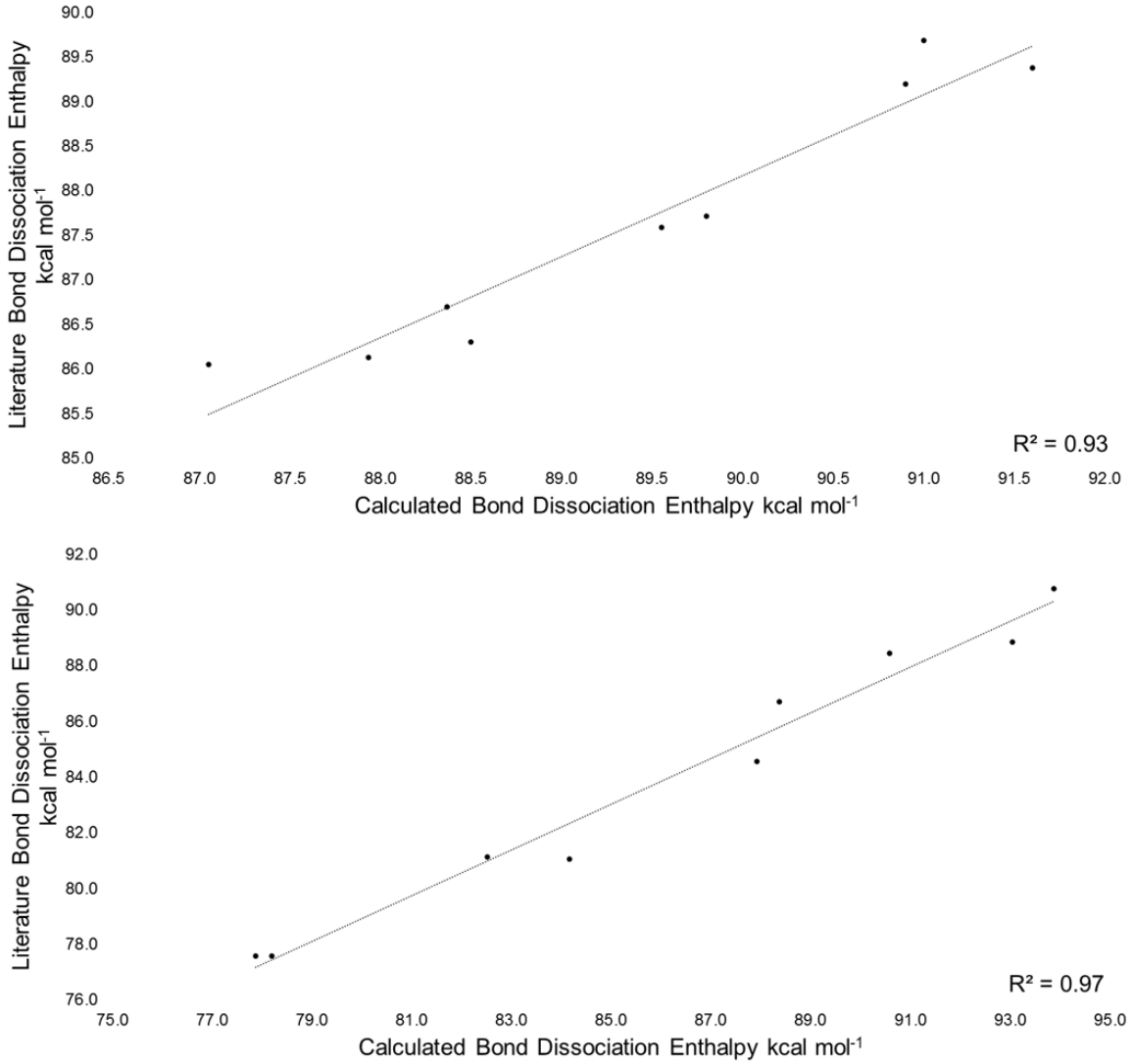

150

151 *Figure 1 Plot of calculated BDEs against mean experimental values taken from* [47] *for the O-H bond*

152 *in meta- and para- substituted phenols*

153 **3. Results and Discussion**

154 Eight typical bond types existing in phenolic bio-oil compounds were selected in this study,

155 they are of the type PhO-CH_3, Ph-OCH_3, PhO-H, Ph-OH, Ph-CH_3, Ph-CHO bonds, Ph-$CHCHCH_3$ and

156 PhCHCH-CH_3. This covers in total 140 bonds from 27 compounds (as shown in Table 2), which are

157 most commonly encountered phenolic bio-oil compounds in the literature [2][49].

158 *Table 2 Phenolic species selected for this study.*

Nº	Compound Name	Structure	Nº	Compound Name	Structure
1	phenol		15	catechol	
2	2-methylphenol		16	guaiacol	
3	4-methylphenol		17	isoeugenol	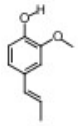
4	2,4-dimethylphenol		18	3-methyl-1,2-benzenediol	
5	2,6-dimethylphenol		19	5-hydroxyvanillin	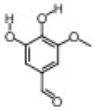
6	2-methoxy-4-methylphenol		20	2,4-dimethoxyphenol	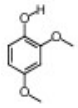
7	2-methoxy-5-methylphenol		21	2,4,6-trimethylphenol	
8	3-methoxy-2,5,6-trimethylphenol		22	3,4,5-trihydroxytoluene	
9	3-methoxy-5-methylphenol		23	pyrogallol	
10	3-methoxy-1,2-benzenediol		24	syringaldehyde	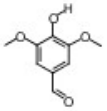
11	2,6-dimethoxthy-4-(1-propenyl)phenol	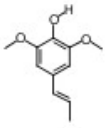	25	syringol	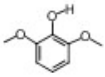
12	2,6-dimethyl-4-(1-propenyl)phenol	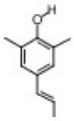	26	6-hydroxy-4-methoxy-2,3-dimethyl-benzaldehyde	
13	3,5-dimethyl-4-hydroxy-benzaldehyde	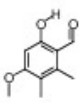	27	3,4,5-trimethylphenol	
14	vanillin	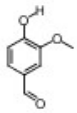			

3.1 Analysis on thermal stability of each bond type

3.1.1 PhO-CH_3

Figure 2 shows the BDEs for all of the methoxy O-CH_3 bonds. It is clear that intramolecular hydrogen bonding plays a critical role in influencing O-CH_3 bond enthalpies. All but two of the lowest energy BDEs up to compound **19**, exhibit hydrogen bonding between the hydrogen atom of the hydroxy group and the oxygen atom of the methoxy group. It is likely that this interaction acts to stabilise the oxyradical species formed following cleavage of the methyl group. We estimate that this hydrogen bonding interaction leads to an increase in BDE of around 5 kcal mol^{-1} by comparing to two methoxy groups in compound **25**.

The location and identity of substituent groups on the ring has a large impact upon the O-CH_3 BDEs. For example, there are three instances in which the effect of an additional methoxy group on carbon 6 can be observed, as seen when comparing compounds **17** and **11**, **16** and **25**, and **14** and **24**. In all three cases, the presence of this extra methoxy group has a minimal impact on the PhO-CH_3 bond enthalpy, reducing it by less than 0.3 kcal mol^{-1}. Compound **19** has an additional hydroxy group on carbon 6 and we can see that, when compared to compound **14**, the presence of this group only leads to a small increase in the O-CH_3 BDE. This can also be observed between compounds **16** and **10**. The BDE increase is slightly more pronounced in the latter example, rising by 1.04 kcal mol^{-1}, however the effect is still relatively small. Based on this, oxygen bearing functional groups can be considered to have little impact upon O-CH_3 BDEs when found in the *para*- position, with respect to the bond of interest. Interestingly, the highest BDE observed in our set is found in compound **26**. This high O-CH_3 BDE is mostly likely caused by the relative position of the methoxy group being found *meta*- to the hydroxy group. This notion is furthered by considering compounds **8** and **9**, which have methoxy groups *meta*- to a hydroxy and which both exhibit high BDE values. The effect of an additional methoxy on the carbon 4 is also more pronounced than on carbon 6. Comparing the energies of the equivalent O-CH_3 bonds on compounds **16** and **20**, we observe a significant decrease in BDE in the latter compound. Non-oxygenated functional groups also lead to shifts in BDEs and, as with the oxygenated groups, the effect is quite variable. Compounds **6** and **7** can both be considered methyl substituted guaiacols, with the methyl group found at the fifth and fourth carbons, respectively. The shift in BDE caused by the

changing methyl group position is rather minimal at 0.24 kcal mol^{-1} and the both compounds exhibit lower O-CH_3 bond enthalpies than unsubstituted guaiacol (**16**) by less than 1.5 kcal mol^{-1}. The presence of multiple methyl groups appears to lower the O-CH_3 bond enthalpy more considerably, as can be seen when comparing compounds **8** and **9**. The two extra methyl groups, on carbons 2 and 6, lead to a reduction in the BDE of 4.18 kcal mol^{-1}. The presence of the propenyl chain on compounds **11** and **17** acts to lower the O-CH_3 BDE found on carbon 2 by slightly over 1 kcal mol^{-1} in both instances. Conversely, the O-CH_3 BDE of the methoxy group at carbon 6 is increased partially by the propenyl chain. In all instances, the formyl group on carbon 4 increases the O-CH_3 bond enthalpy. For the methoxy group on carbon 2, this increase is over 4 kcal mol^{-1}.

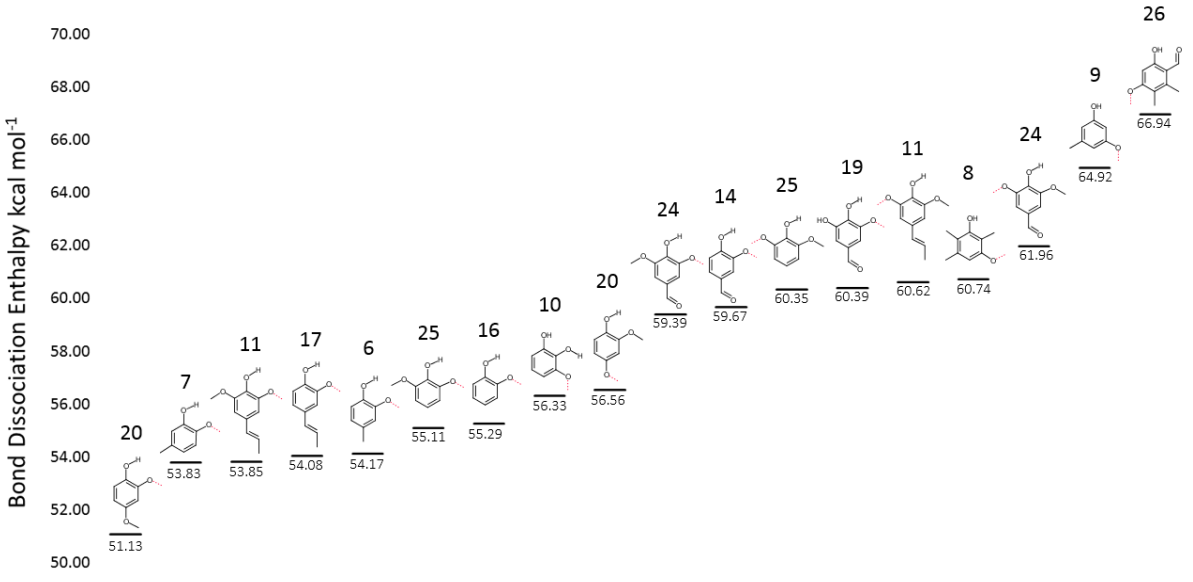

Figure 2 BDEs for all methoxy PhO-CH3 bonds. The measured bond is represented by a dashed red line.

Overall, whilst there is considerable variation amongst the O-CH_3 BDEs in these compounds, the influence of any particular substituent group, and its relative location, are difficult to define. Nevertheless, the effect of hydrogen bonding in reducing O-CH_3 BDEs is clear. Furthermore, the placement of oxygen bearing functional groups *meta-* to the bond of interest most likely leads to elevated BDEs.

3.1.2 Ph-OCH_3

The BDEs for all Ph-OCH_3 bonds are shown in Figure 3. It is quite apparent that the Ph-OCH_3 BDEs are found within a much smaller range than those for the O-CH_3 bonds. This suggest that substituent groups have notably less influence on the stability of radicals found directly on the benzene ring than when the unpaired electron is located on an oxygen atom.

Again, the role of hydrogen bonding is relatively straightforward. The weakest BDEs are found in compounds in which no hydrogen bonding is observed between the hydroxy hydrogen and the methoxy group of interest. Ten of the highest eleven bonds are found on compounds in which cleaving the Ph-O bond would eliminate a hydrogen bond. The exception to this trend is compound **26** which may have an elevated BDE owing to the presence of the formyl group on the ring. This is supported by the fact that the three highest BDE compounds also have formyl groups. The reason for the increased BDEs in unclear but may be caused by the electron withdrawing nature of the formyl group causing a wider distribution of the electron density, leading to stabilisation of the radical species.

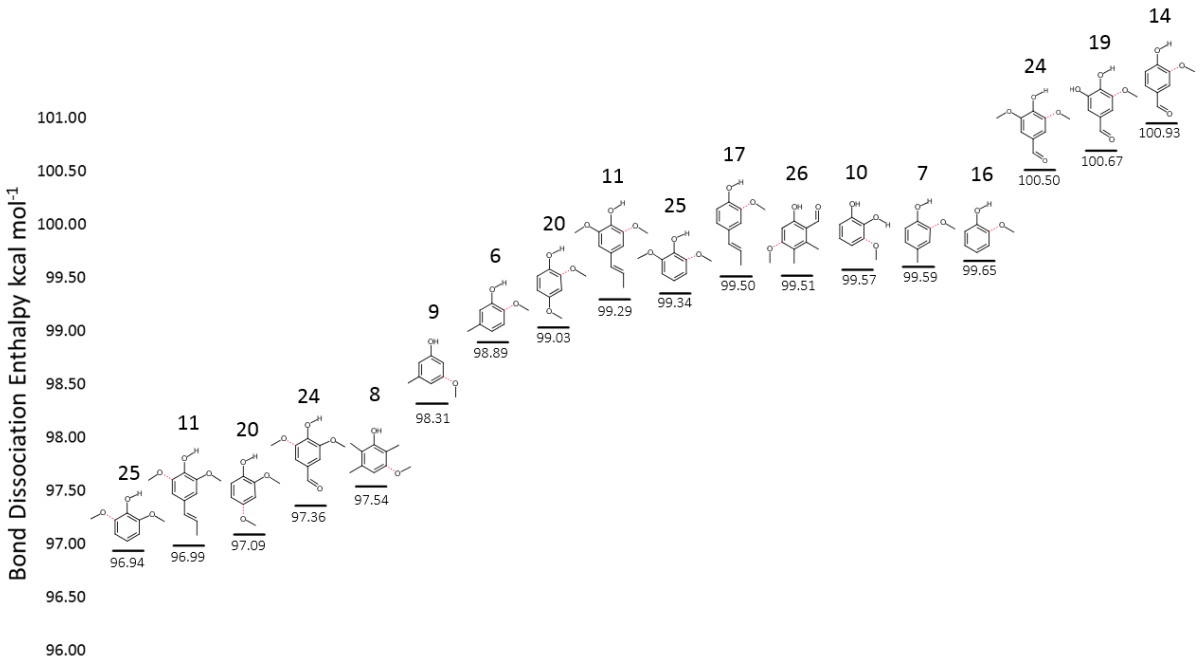

Figure 3 BDEs for all methoxy Ph-OCH3 bonds. The measured bond is represented by a dashed red line.

Whilst no longer presented as pairs in Figure 3 as they are in Figure 2, compounds **11** and **17**, **16** and **25**, and **14** and **24** all still highlight the sub-kcal reduction in BDE that is caused by the addition of a methoxy group on sixth carbon. Furthermore, addition of a methoxy to the fourth carbon also leads

to only a minor reduction in the Ph-OCH_3 BDE. Looking at compounds **6** and **7** we can infer what influence the position of a methyl group has. As with the O-CH_3 bond strengths, compound **7**, where the methyl group is on the fourth carbon, exhibits the higher bond strength, although in this case the increase in bond enthalpy is a modest 0.70 kcal mol^{-1}. In both instances, the BDE is lower than unsubstituted guaiacol (**16**). Furthermore, comparing compounds **8** and **9**, we can see that the further addition of methyl groups leads to a greater reduction in the BDE. It is also interesting to note that the propenyl chains have little impact on the BDE of the methoxy groups found on the second carbon, reducing the bond enthalpies by just 0.15 kcal mol^{-1} at most. In regards to the methoxy group on the sixth carbon, comparing compounds **11** and **25** shows that the propenyl chain slightly increases the Ph-OCH_3 BDE, however, this change in value is small enough to be considered negligible.

We observe practically zero correlation between the PH-OCH3 and O-CH3 bond enthalpies for each compound, further positing the idea that the ring based radical requires alternative stabilisation routes than the oxygen centred radical. As with the O-CH_3 bonds, hydrogen bonding has a large influence on the strength of Ph-OCH_3 bonds, however, the trend here is reversed, with hydrogen bonded compounds exhibiting higher BDEs. As compound **16** has a relatively high BDE, this suggests a general trend that substitution of guaiacol leads to reductions in the Ph-OCH_3 BDE.

3.1.3 Ph-CH_3

In total 26 Ph-CH3 bonds were calculated, which are shown in Figures **4** and **5**. All bonds were found within relatively large range, the lowest being 99.03 kcal mol^{-1} and the largest was 106.83 kcal mol^{-1}. It was found that the Ph-CH3 bonds exhibit a complicated relationship with respect to substitution patterns. One noticeable trend is that six of the lowest seven BDEs are found on groups which are *ortho-* with respect to another methyl group. An additional methyl group on the *meta-* position leads to irregular changes in BDE. Comparing compound **4** in Figure 4 to compound **2** in Figure 5, we see a significant drop in the Ph-CH_3 bond energy, yet conversely comparing compounds **3** and **4** in Figure 5, we see that the addition of the methyl in the *meta-* position leads to an increase in BDE of almost 2 kcal mol^{-1}. The methyl group being positioned *ortho-* or *para-* to a hydroxy group tends to yield higher BDEs, whilst those found *ortho-* to hydroxy groups have lower bond enthalpies. Unlike the methoxy

group compounds presented in Figures 2 and 3, the presence of a formyl group does not lead to significantly increased bond strengths.

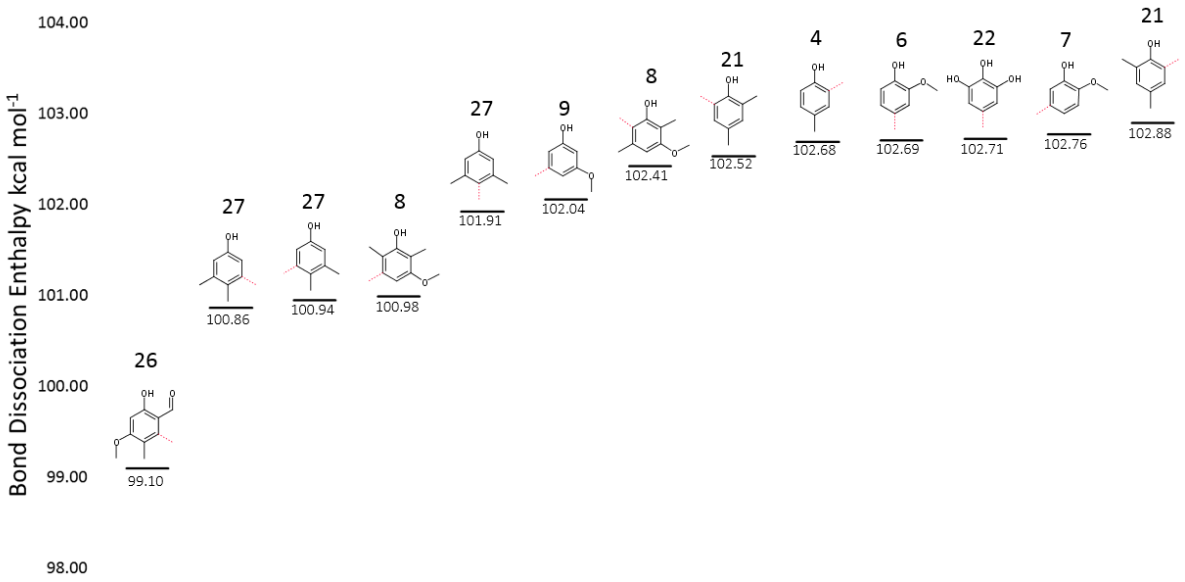

Figure 4 BDEs for the lower 12 Ph-CH3 bonds. The measured bond is represented by a dashed red line.

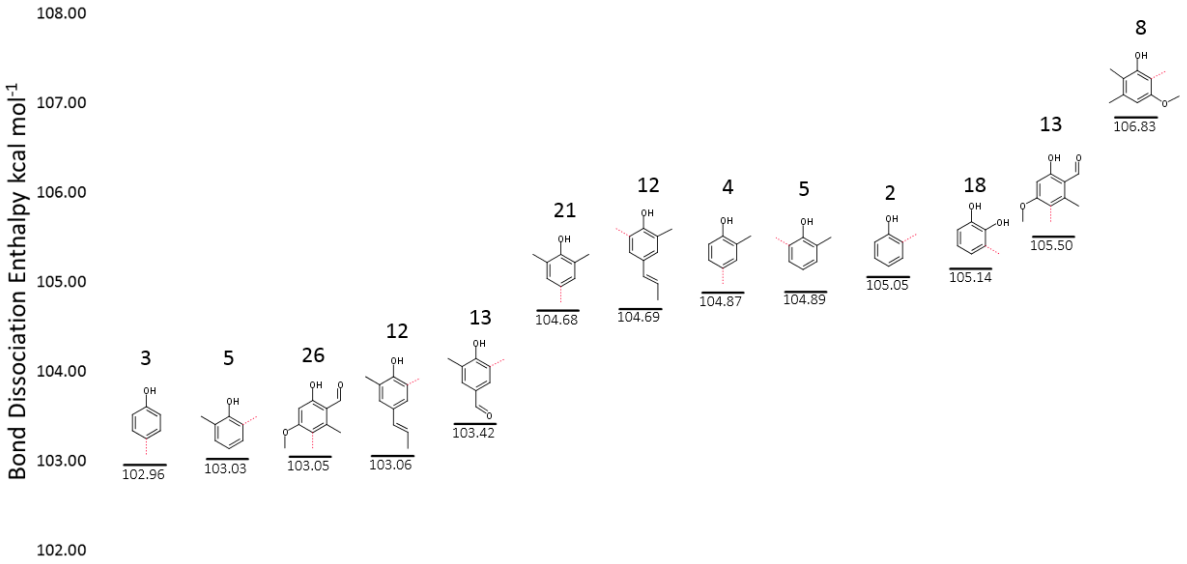

Figure 5 BDEs for the higher 12 Ph-CH3 bonds. The measured bond is represented by a dashed red line.

Compound **8** exhibits the highest Ph-CH_3 BDE, which is most likely due to the methyl group being located adjacent to two strongly electron donating groups. Generally, the highest BDEs all have strong electron donating groups in either the *ortho-* or *para-* positions, which may explain the higher

bond enthalpies. Of all the methyl phenols, the singly substituted 2-methyl phenol has the highest BDE, and additional methyl substitution on the other carbons leads to a reduction in bond enthalpy.

3.1.4 PhO-H

All phenoxy O-H bonds are given in Figures 6 and 7. These bonds exhibited the largest range of any bond type in this study. As with the O-CH_3 bonds presented earlier, hydrogen bonding plays an important role in altering the O-H BDEs. A key feature of many of the lower BDEs is that the oxyradical resulting from a bond cleavage is stabilised through hydrogen bonding to a neighbouring hydroxy group. Comparing compound **19** in Figure 6 with compound **14** in Figure 7 gives some indication as to the stabilising effect of this hydrogen bonding interaction, with the O-H BDE decreasing almost 9 kcal mol^{-1} when the stabilising hydrogen bond is present. The highest energy O-H bond is found in compound **26**, with a BDE of 99.93 kcal mol^{-1}, almost 12 kcal mol^{-1} higher than the nearest value. The reasons for this are likely twofold. Firstly, the strong hydrogen bonding interaction between the hydrogen atom and adjacent formyl group may act to stabilise the compound and bind the hydrogen atom. Secondly, following the cleavage of the O-H bond, the newly formed species exhibits considerable repulsion between the radical oxygen atom and the oxygen of the formyl group.

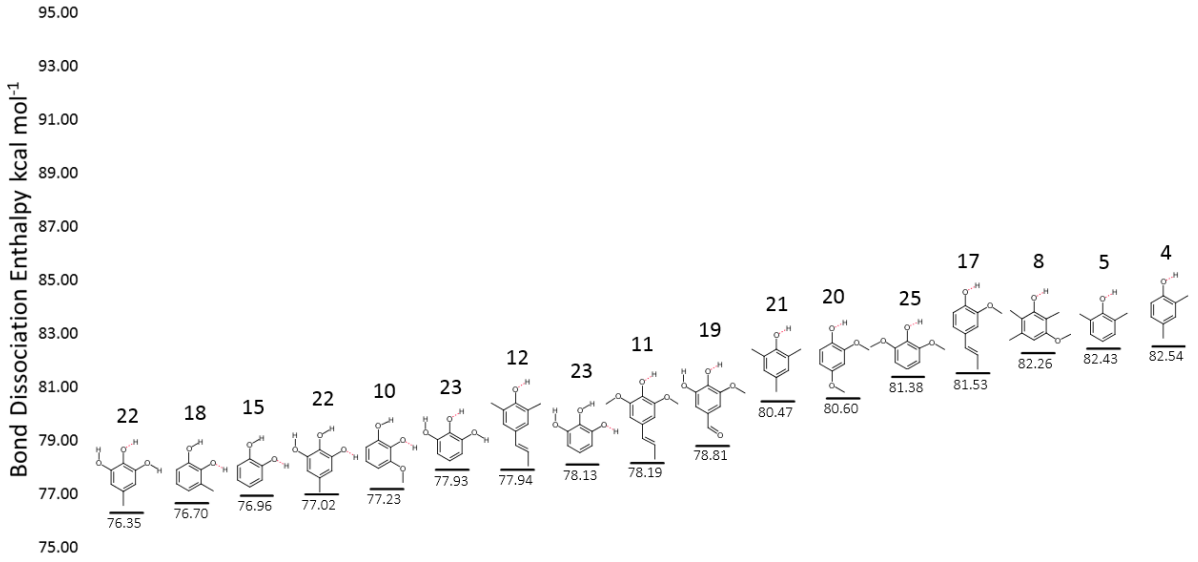

Figure 6 BDEs for the lower 17 phenolic O-H bonds. The measured bond is represented by a dashed red line.mol^{-1}.

Exactly what effect the addition of methyl groups has upon the O-H BDEs is difficult to discern, however, when we compare the methylated phenols, compounds **2**, **3**, **4**, **5** and **27**, against unsubstituted phenol, we see that the presence of 1 or more methyl groups lowers the O-H BDE by at least 2.11 kcal

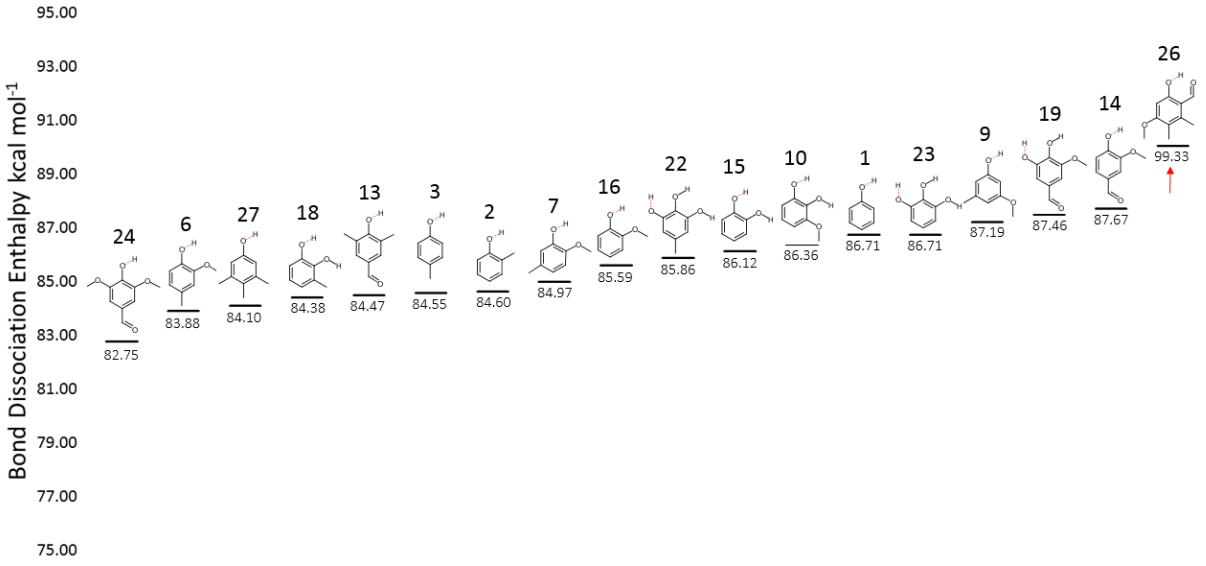

Figure 7 BDEs for the higher 18 phenolic O-H bonds. The measured bond is represented by a dashed red line.

The trivial difference in BDE between compounds **4** and **5** and also between compounds **2** and **3** suggest that substitution with methyl groups on either the *ortho-* (**2** and **5)** or *para-* (**3** and **4**) positions leads to practically identical changes in O-H BDE. The bond enthalpy of compound **7** is 0.62 kcal mol^{-1} lower than compound **16**, suggesting that methyl substitution *meta-* to the hydroxy leads to a lowering of the bond enthalpy. The bond enthalpies of species containing a propenyl group are all relatively low and conversely, the presence of formyl groups increases bond enthalpies such that the three highest BDEs are found in formyl containing compounds. The wide ranging values for O-H bond enthalpies is reminiscent of those presented earlier for the O-CH_3 bonds. This provides further evidence that the stability of the oxyradical is highly dependent on the substitution pattern on the ring. Unsubstituted phenol (**1**) has a relatively high O-H bond enthalpy, indicating that, like was observed for the guaiacol (**16**) O-CH_3 bond, additional substitution will, in general, lower the O-H BDE.

3.1.5 Ph-OH

The phenolic Ph-OH bonds are given in Figures 8 and 9. All bonds exhibited high strength, ranging from 109.66 kcal mol^{-1} to 121.57 kcal mol^{-1}. As was the case for the O-H bonds, the highest

observed BDE is found on compound **26**. We propose that this high bond strength is caused by hydrogen bonding with the neighbouring formyl group. The effect of hydrogen bonding interactions is most apparent in Ph-OH bonds and follows a clear trend. We observe that all of the lowest BDEs are found on non-hydrogen bonded functional groups, which are flanked by either hydrogens or methyl groups. The only exception to this is found in compound **13**, which has a BDE of 113.29 kcal mol^{-1}. The OH group in this species is found *para*- to the strongly electron donating formyl group, which may likely explain the higher BDE. Following the non-hydrogen bonding compounds, we find those in which only the oxygen atom participates in the hydrogen bonding are the next strongest type of Ph-OH bond, as seen in compounds **22**, **18**, **15** and **23**. Following these, the next strongest BDEs are found on the compounds in which only the hydrogen atom is engaged in hydrogen bonding with neighbouring groups. This style of hydrogen bonding gives rise to BDEs that are around 1 kcal mol^{-1} stronger than the previous group. This effect can be seen in pyrogallol (**23**), in which the hydroxy groups on either side of the molecule have Ph-OH BDEs that differ by 1.75 kcal mol^{-1}. Again, the presence of a formyl group *para*- with respect to the OH group leads to a deviation from this trend, with compounds **24** and **14** having partially elevated BDEs. The highest BDEs measured, with the exception of compounds **26**, **14** and **24**, are found where the cleaved O-H group is engaged in hydrogen bonding, both at the hydrogen atom and the oxygen atom. Cleavage of this group leads to a radical that has no intramolecular hydrogen bonds, which would in turn give rise to higher instability in the radical species.

All methyl phenols are found within a small range around unsubstituted phenol (**1**) in Figure 8. The relationship between methyl substitution and shifting BDE is rather erratic, however it would appear that substitution at the *ortho*- position has a strengthening effect, whilst *meta*- and *para*-substitution lead to reductions in the Ph-OH BDE. In all instances it would appear that methyl substitution has a relatively small impact upon the strength of the Ph-OH bond. The presence of the propenyl chain on the fourth carbon increases the BDE, see compounds **5** and **12**, **25** and **11**, and **16** and **17**, but the effect is quite minimal and energy increases are 0.35 kcal mol^{-1} or less. Furthermore, addition of a non-hydrogen bonding methoxy group lowers the O-H BDE by around 1.15 kcal mol^{-1} as shown by compounds **16** and **25**, and compounds **17** and **11**.

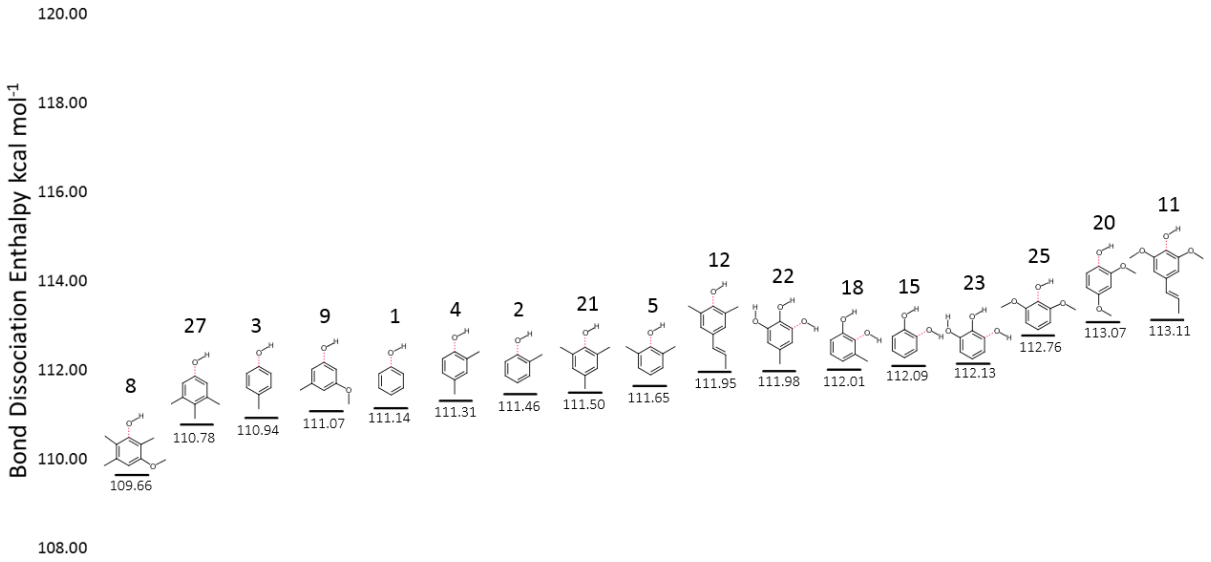

Figure 8 BDEs for the lower 17 phenolic Ph-OH bonds. The measured bond is represented by a dashed red line.

Considering compounds **8** to **12** in Figure 8, including unsubstituted phenol (**1**) it is clear that the addition of multiple functional groups on the ring has a minimal impact upon the Ph-OH BDE. Additionally, as was the case for the methoxy group bonds, we observe almost nil correlation between the Ph-O bond enthalpy and the corresponding O-H bond.

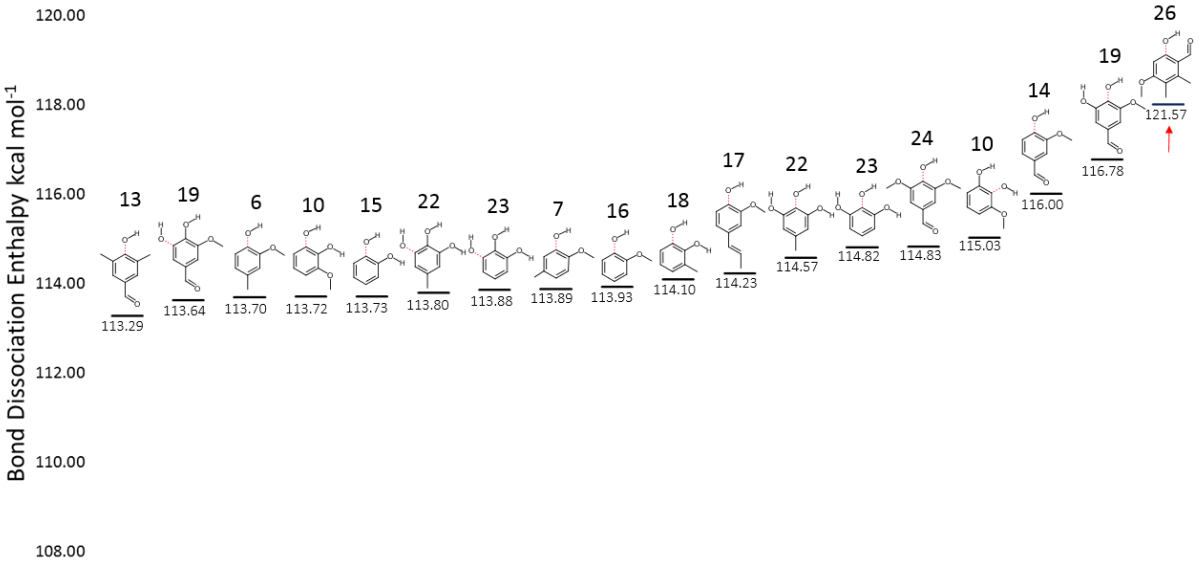

Figure 9 BDEs for the higher 18 phenolic Ph-OH bonds. The measured bond is represented by a dashed red line

3.1.6 Ph-CHO

There were only three formyl groups in the compounds in this study and their bonds enthalpies are provided, together with those for the propenyl groups, in Figure 10. The Ph-CHO values are similar in strength to those for the Ph-CH3 bonds. The BDE for compound **26** is considerably higher than for the other to formyl containing compounds and this is most likely caused by the interaction of the carbonyl oxygen with the neighbouring hydroxy group. Cleavage of the formyl substituent would also interrupt this hydrogen bond and this leads to the increased BDE. Addition of the extra methoxy group on the sixth carbon leads to a reduction in BDE of 0.42 kcal mol^{-1}, a similar shift in strength to that which is observed for the other bond types.

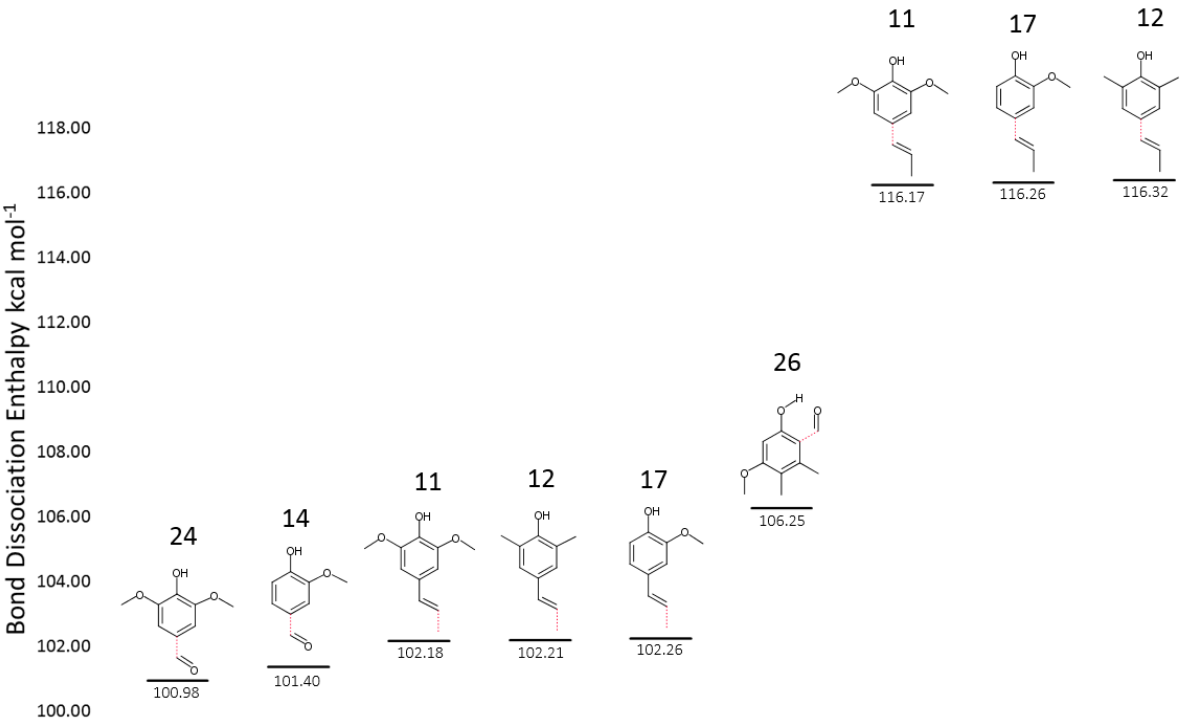

Figure 10 BDEs for the 3 Ph-CHO bonds, 3 Ph-CHCHCH$_3$ bonds and 3 PhCHCH-CH$_3$ bonds. The measured bond is represented by a dashed red line.

3.1.7 PhCHCH-CH$_3$

It is interesting to find that the three BDEs required for cleavage of a methyl group from a propenyl chain are all found within 0.06 kcal mol^{-1} of each other (shown in Figure 10). This suggests that the variable substituent groups upon the ring have little effect on stabilisation of the radical species.

As with the formyl group bond enthalpies, the addition of the second methoxy group lowers the bond enthalpy, however, the change is almost negligible.

3.1.8 Ph-CHCHCH$_3$

As with the PhCHCH-CH$_3$ bonds, the BDEs for cleavage of the entire propenyl chain fall within a very narrow range, from 116.17 kcal mol^{-}1 to 116.32 kcal mol^{-}1 (shown in Figure 10). These are the highest BDEs of any compound in this study, and we may ascribe the high dissociation energy of these bonds to significant conjugation between the propenyl chain and the benzene ring.

3.2 Comparison to experimental observations

Table 3 shows the BDE range of each bond type reported in this work, highlighting the large variation in bond strengths between the different functional groups

Table 3 BDE ranges for the seven different bond types assessed within this study.

Bond Type	PhO-CH3	Ph-OCH3	Ph-CH3	PhO-H	Ph-OH	Ph-CHO	PhCHCH-CH3	Ph-CHCHCH3
BDE Range (kcal mol^{-1})	51.13-66.94	96.94-100.93	99.10-106.83	76.35-99.33	109.66-121.57	100.98-106.25	102.18-102.26	116.17-116.32

The calculations in this work reflected that the methoxy O-CH$_3$ bond is relatively weaker than the other bond types. This trend correlates well with the observations of experimental works. This also, in part, explains the significant reduction in methoxy containing compounds observed following higher temperature pyrolysis. Jiang et al. [49] reported that the total yield and relative concentrations of methoxy phenols was reduced at the higher reaction temperature of 800 ^{O}C. Similar trends in the loss of methoxy groups were also found by Shafaghat et al. [12] and by Shao et al. [13]. As the methoxy O-CH$_3$ bond is significantly weaker than the bond between the ring and the methoxy oxygen, cleavage of the former will be occur at a much higher rate, meaning that the strength of the Ph-OCH$_3$ bond will have little impact upon the thermal stability of a compound.

The O-H bonds of the hydroxy groups are also weak in relation to the other bonds calculated. From this information one might assume that this would lead to lower thermal stabilities of phenolic compounds, however, it is likely that recombination of oxyradicals with prevalent hydrogen radicals would lead to reformation of hydroxy groups. Therefore, thermal degradation on O-H bonds is unlikely to alter the identity of a detected species. Conversely, if a Ph-OH bond were to rupture, the product

compound would likely be altered. Phenolic species are present in significant quantities following higher temperature pyrolysis, see Jiang et al. [49] and Shafaghat et al. [12], suggesting that the range of bond enthalpies for Ph-OH bonds presented here are sufficiently large enough as to be thermally stable at elevated temperatures.

The three bonds types, Ph-CH_3, Ph-CHO and PhCHCH-CH3, all have similar values for their BDEs and all generally exhibit stable concentrations at high pyrolysis temperatures.

4. Conclusions

In this work we have presented BDEs for a range of phenolic compounds identified in bio-oil. An initial method comparison study identified the PW6B95 functional as the most accurate for calculation of BDEs in relation to seven common aromatic substituent groups. Further validation of our chosen method, through calculation of O-H BDEs for substituted phenols, highlighted its applicability for modelling the influence of aromatic substituent groups.

The weakest bond within the eight selected phenolic bio-oil bond types was the methoxy PhO-CH_3, the values of which are found within the range of 51.13 to 66.94 kcal mol^{-1}. Next weakest was the hydroxy PhO-H bonds, ranging from 76.35 to 99.33 kcal mol^{-1}. The methoxy Ph-OCH_3 bonds were found within a small distribution, from 96.94 to 100.93 kcal mol^{-1} and their relative weakness may in part explain the low thermal stability of methoxy phenol compounds such as guaiacol and syringol. The Ph-CH_3, Ph-CHO and PhCHCH-CH_3 all had similar bond strengths values in excess of 100 kcal mol^{-1} and all are found following increased temperature pyrolysis experiments. Lastly, the Ph-OH and Ph-$CHCHCH_3$ bonds all exhibited high strengths, which correlates well with increased concentrations of phenol and styrene following high temperature pyrolysis. Furthermore, based on the wide ranges observed for the PhO-H and PhO-CH_3 BDEs, we conclude that the stability of aromatic oxyradicals is highly dependent upon the identity of substituent groups on the benzene ring.

Acknowledgements

Financial support from the Department for the Economy (Northern Ireland, United Kingdom) for the Ph.D. research of A. Shaw is gratefully acknowledged. The authors also would like to

403 acknowledge the support from Leverhulme Trust Research Grant (RPG-2017-254) and EPSRC (The
404 Engineering and Physical Sciences Research Council, the United Kingdom) First Grant
405 (EP/R010986/1).

406 **References**

407 [1] International Energy Agency. Key World Energy Statistics. 2018.

408 [2] Luo Z, Wang S, Liao Y, Zhou J, Gu Y, Cen K. Research on biomass fast pyrolysis for liquid
409 fuel. Biomass and Bioenergy 2004;26:455–62. doi:10.1016/j.biombioe.2003.04.001.

410 [3] Branca C, Giudicianni P, Di Blasi C. GC/MS characterization of liquids generated from low-
411 temperature pyrolysis of wood. Ind Eng Chem Res 2003;42:3190–202. doi:10.1021/ie030066d.

412 [4] Salehi E, Abedi J, Harding T. Bio-oil from sawdust: Effect of operating parameters on the yield
413 and quality of pyrolysis products. Energy and Fuels 2011;25:4145–54. doi:10.1021/ef200688y.

414 [5] Bridgwater A V. Review of fast pyrolysis of biomass and product upgrading. Biomass and
415 Bioenergy 2012;38:68–94. doi:10.1016/j.biombioe.2011.01.048.

416 [6] Zhang X, Yang W, Blasiak W. Modeling study of woody biomass: Interactions of cellulose,
417 hemicellulose, and lignin. Energy and Fuels 2011;25:4786–95. doi:10.1021/ef201097d.

418 [7] Wang S, Ru B, Lin H, Sun W. Pyrolysis behaviors of four O-acetyl-preserved hemicelluloses
419 isolated from hardwoods and softwoods. Fuel 2015;150:243–51.
420 doi:10.1016/j.fuel.2015.02.045.

421 [8] Gibson LJ. The hierarchical structure and mechanics of plant materials. J R Soc Interface
422 2012;9:pp 2749-2766. doi:10.1098/rsif.2012.0341.

423 [9] Patwardhan PR, Brown RC, Shanks BH. Product distribution from the fast pyrolysis of
424 hemicellulose. ChemSusChem 2011;4:636–43. doi:10.1002/cssc.201000425.

425 [10] Wang S, Guo X, Liang T, Zhou Y, Luo Z. Mechanism research on cellulose pyrolysis by Py-
426 GC/MS and subsequent density functional theory studies. Bioresour Technol 2012;104:722–8.

427 doi:10.1016/j.biortech.2011.10.078.

428 [11] Huang J, Liu C, Tong H, Li W, Wu D. A density functional theory study on formation
429 mechanism of CO, CO2 and CH4 in pyrolysis of lignin. Comput Theor Chem 2014;1045:1–9.
430 doi:10.1016/j.comptc.2014.06.009.

431 [12] Shafaghat H, Rezaei PS, Ro D, Jae J, Kim BS, Jung SC, et al. In-situ catalytic pyrolysis of lignin
432 in a bench-scale fixed bed pyrolyzer. J Ind Eng Chem 2017;54:447–53.
433 doi:10.1016/j.jiec.2017.06.026.

434 [13] Shao L, Zhang X, Chen F, Xu F. Fast pyrolysis of Kraft lignins fractionated by ultrafiltration. J
435 Anal Appl Pyrolysis 2017:0–1. doi:10.1016/j.jaap.2017.11.003.

436 [14] Chen L, Ye X, Luo F, Shao J, Lu Q, Fang Y, et al. Pyrolysis mechanism of β-O-4 type lignin
437 model dimer. J Anal Appl Pyrolysis 2015;115:103–11. doi:10.1016/j.jaap.2015.07.009.

438 [15] Zhang JJ, Jiang XY, Ye XN, Chen L, Lu Q, Wang XH, et al. Pyrolysis mechanism of a β-O-4
439 type lignin dimer model compound: A joint theoretical and experimental study. J Therm Anal
440 Calorim 2016;123:501–10. doi:10.1007/s10973-015-4944-y.

441 [16] Horne PA, Williams PT. Influence of temperature on the products from the flash pyrolysis of
442 biomass. Fuel 1996;75:1051–9. doi:10.1016/0016-2361(96)00081-6.

443 [17] Li J, Yan R, Xiao B, Wang X, Yang H. Influence of temperature on the formation of oil from
444 pyrolyzing palm oil wastes in a fixed bed reactor. Energy and Fuels 2007;21:2398–407.
445 doi:10.1021/ef060548c.

446 [18] Ates F, Isikdag MA. Evaluation of the role of the pyrolysis temperature in straw biomass
447 samples and characterization of the oils by GC/MS. Energy and Fuels 2008;22:1936–43.
448 doi:10.1021/ef7006276.

449 [19] Lu Q, Yang XC, Dong CQ, Zhang ZF, Zhang XM, Zhu XF. Influence of pyrolysis temperature
450 and time on the cellulose fast pyrolysis products: Analytical Py-GC/MS study. J Anal Appl
451 Pyrolysis 2011;92:430–8. doi:10.1016/j.jaap.2011.08.006.

[20] Muller P. Glossary of Terms Used in Physical Organic Chemistry. Pure Appl Chem 1994;66:1077–184. doi:10.1351/pac199466051077.

[21] Brinck T, Haeberlein M, Jonsson M. A computational analysis of substituent effects on the O-H bond dissociation energy in phenols: Polar versus radical effects. J Am Chem Soc 1997;119:4239–44. doi:10.1021/ja962931+.

[22] Klein E, Lukeš V. DFT/B3LYP study of O-H bond dissociation enthalpies of para and meta substituted phenols: Correlation with the phenolic C-O bond length. J Mol Struct THEOCHEM 2006;767:43–50. doi:10.1016/j.theochem.2006.04.017.

[23] Marteau C, Guitard R, Penverne C, Favier D, Nardello-Rataj V, Aubry JM. Boosting effect of ortho-propenyl substituent on the antioxidant activity of natural phenols. Food Chem 2016;196:418–27. doi:10.1016/j.foodchem.2015.09.007.

[24] Richard LS, Bernardes CES, Diogo HP, Leal JP, Da Piedade MEM. Energetics of cresols and of methylphenoxyl radicals. J Phys Chem A 2007;111:8741–8. doi:10.1021/jp073515m.

[25] Prasomsri T, Shetty M, Murugappan K, Román-Leshkov Y. Insights into the catalytic activity and surface modification of MoO_3 during the hydrodeoxygenation of lignin-derived model compounds into aromatic hydrocarbons under low hydrogen pressures. Energy Environ Sci 2014;7:2660–9. doi:10.1039/C4EE00890A.

[26] Kim S, Chmely SC, Nimlos MR, Bomble YJ, Foust TD, Paton RS, et al. Computational study of bond dissociation enthalpies for a large range of native and modified Lignins. J Phys Chem Lett 2011;2:2846–52. doi:10.1021/jz201182w.

[27] Elder T. Bond dissociation enthalpies of a dibenzodioxocin lignin model compound. Energy and Fuels 2013;27:4785–90. doi:10.1021/ef401026g.

[28] Elder T. Bond dissociation enthalpies of a pinoresinol lignin model compound. Energy and Fuels 2014;28:1175–82. doi:10.1021/ef402310h.

[29] Parthasarathi R, Romero RA, Redondo A, Gnanakaran S. Theoretical study of the remarkably

diverse linkages in lignin. J Phys Chem Lett 2011;2:2660–6. doi:10.1021/jz201201q.

[30] Neese F. Software update: the ORCA program system, version 4.0. Wiley Interdiscip Rev Comput Mol Sci 2018;8. doi:10.1002/wcms.1327.

[31] Hemelsoet K, Van Speybroeck V, Van Geem KM, Marin GB, Waroquier M. Using elementary reactions to model growth processes of polyaromatic hydrocarbons under pyrolysis conditions of light feedstocks. Mol Simul 2008;34:193–9. doi:10.1080/08927020801930588.

[32] O'Reilly RJ, Karton A. A dataset of highly accurate homolytic NBr bond dissociation energies obtained by Means of W2 theory. Int J Quantum Chem 2016;116:52–60. doi:10.1002/qua.25024.

[33] Oyeyemi VB, Dieterich JM, Krisiloff DB, Tan T, Carter EA. Bond dissociation energies of C10 and C18 methyl esters from local multireference averaged-coupled pair functional theory. J Phys Chem A 2015;119:3429–39. doi:10.1021/jp512974k.

[34] Zhao Y, Truhlar DG. The M06 suite of density functionals for main group thermochemistry, thermochemical kinetics, noncovalent interactions, excited states, and transition elements: Two new functionals and systematic testing of four M06-class functionals and 12 other function. Theor Chem Acc 2008;120:215–41. doi:10.1007/s00214-007-0310-x.

[35] Stephens PJ, Devlin FJ, Chabalowski CF, Frisch MJ. Ab Initio Calculation of Vibrational Absorption and Circular Dichroism Spectra Using Density Functional Force Fields. J Phys Chem 1994;98:11623–7. doi:10.1021/j100096a001.

[36] Adamo C, Barone V. Toward reliable density functional methods without adjustable parameters: The PBE0 model. J Chem Phys 1999;110:6158–70. doi:10.1063/1.478522.

[37] Zhao Y, Truhlar DG. Design of density functionals that are broadly accurate for thermochemistry, thermochemical kinetics, and nonbonded interactions. J Phys Chem A 2005;109:5656–67. doi:10.1021/jp050536c.

[38] Becke AD. Density-functional thermochemistry. III. The role of exact exchange. J Chem Phys

1993;98:5648. doi:10.1063/1.464913.

[39] Perdew JP, Wang Y. Accurate and simple analytic representation of the electron-gas correlation energy. Phys Rev B 1992;45:13244–9. doi:10.1103/PhysRevB.45.13244.

[40] Weigend F, Ahlrichs R. Balanced basis sets of split valence, triple zeta valence and quadruple zeta valence quality for H to Rn: Design and assessment of accuracy. Phys Chem Chem Phys 2005;7:3297. doi:10.1039/b508541a.

[41] Weigend F. Accurate Coulomb-fitting basis sets for H to Rn. Phys Chem Chem Phys 2006;8:1057. doi:10.1039/b515623h.

[42] Grimme S, Antony J, Ehrlich S, Krieg H. A consistent and accurate ab initio parametrization of density functional dispersion correction (DFT-D) for the 94 elements H-Pu. J Chem Phys 2010;132. doi:10.1063/1.3382344.

[43] Grimme S, Ehrlich S, Goerigk L. Effect of the damping function in dispersion corrected density functional theory. J Comput Chem 2011;32:1456–65. doi:10.1002/jcc.21759.

[44] Goerigk L, Hansen A, Bauer CA, Ehrlich S, Najibi A, Grimme S. A Look at the Density Functional Theory Zoo with the Advanced GMTKN55 Database for General Main Group Thermochemistry, Kinetics and Noncovalent Interactions. Phys Chem Chem Phys 2017;19:32184–215. doi:10.1039/C7CP04913G.

[45] Neese F, Wennmohs F, Hansen A, Becker U. Efficient, approximate and parallel Hartree-Fock and hybrid DFT calculations. A “chain-of-spheres” algorithm for the Hartree-Fock exchange. Chem Phys 2009;356:98–109. doi:10.1016/j.chemphys.2008.10.036.

[46] Blanksby SJ, Ellison GB. Bond dissociation energies of organic molecules. Acc Chem Res 2003;36:255–63. doi:10.1021/ar020230d.

[47] Luo Y-R. Handbook of Bond Dissociation Energies in Organic Compounds. CRC Press; 2003.

[48] Pople JA. Nobel Lecture: Quantum chemical models. Rev Mod Phys 1999;71:1267–74.

526 doi:10.1103/revmodphys.71.1267.

527 [49] Jiang G, Nowakowski DJ, Bridgwater A V. Effect of the Temperature on the Composition of
528 Lignin Pyrolysis Products. Energy & Fuels 2010;24:4470–5. doi:10.1021/ef100363c.

529